

## ORIGINAL ARTICLE

# SNCA, a novel biomarker for Group 4 medulloblastomas, can inhibit tumor invasion and induce apoptosis

Yong-Xiao Li<sup>1</sup> | Zhen-Wei Yu<sup>1</sup> | Tao Jiang<sup>2</sup> | Li-Wei Shao<sup>1</sup> | Yan Liu<sup>1</sup> | Na Li<sup>1</sup> | Yu-Feng Wu<sup>1</sup> | Chen Zheng<sup>1</sup> | Xiao-Yu Wu<sup>1</sup> | Ming Zhang<sup>1</sup> | Dan-Feng Zheng<sup>1</sup> | Xue-Ling Qi<sup>3</sup> | Min Ding<sup>4</sup> | Jing Zhang<sup>1,5</sup> | Qing Chang<sup>1</sup> 

<sup>1</sup>Department of Pathology, Peking University School of Basic Medical Science, Peking University Third Hospital, Peking University Health Science Center, Beijing, China

<sup>2</sup>Department of Neurosurgery, Beijing Tiantan Hospital, Beijing, China

<sup>3</sup>Department of Pathology, Beijing Sanbo Brain Hospital, Beijing, China

<sup>4</sup>Department of Pathology, Anhui Provincial Hospital, Hefei, China

<sup>5</sup>Department of Pathology, University of Washington, Seattle, WA, USA

**Correspondence**

Qing Chang, Department of Pathology, Peking University School of Basic Medical Science, Peking University Third Hospital, Peking University Health Science Center, Beijing, China.

Email: qingchang@bjmu.edu.cn

**Funding Information**

National Natural Science Foundation of China; Peking University Third Hospital, Peking University Health Science Center.

Medulloblastoma (MB) is the most common malignant brain tumor in childhood. It contains at least four distinct molecular subgroups. The aim of this study is to explore novel diagnostic and potential therapeutic markers within each subgroup of MB, in particular within Group 4, the largest subgroup, to facilitate diagnosis together with gene therapy. One hundred and six MB samples were examined. Tumor subtype was evaluated with the NanoString assay. Several novel tumor related genes were shown to have high subgroup sensitivity and specificity, including *PDGFRA*, *FGFR1*, and *ALK* in the WNT group, *CCND1* in the SHH group, and  $\alpha$ -synuclein (*SNCA*) in Group 4. Knockdown and overexpression assays of *SNCA* revealed the ability of this gene to inhibit tumor invasion and induce apoptosis. Methylation-specific PCR and pyrosequencing analysis showed that epigenetic mechanisms, rather than DNA hypermethylation, might play the key role in the regulation of *SNCA* expression in MB tumors. In conclusion, we identify *SNCA* as a novel diagnostic biomarker for Group 4 MB. Some other subgroup signature genes have also been found as candidate therapeutic targets for this tumor.

**KEYWORDS**

biomarker, medulloblastoma, molecular subtype, *SNCA*, tumor invasion

## 1 | INTRODUCTION

Medulloblastoma (MB) is the most common malignant brain tumor in childhood. A multimodal treatment strategy, with surgical resection followed by radiotherapy and chemotherapy, has improved the overall 5 year-survival rate to >80%, but the prognosis for patients with recurrent MB remains very poor; patients with areas of frank

dissemination had a low 5-year event-free survival rate of approximately 36%.<sup>1,2</sup>

There is now a consensus, based on current studies, including our recent results, that MB is not a single tumor, but is rather a heterogeneous group of tumors that differ not only in histologic appearance, but also in molecular biology. Medulloblastoma can be divided into at least four clinically, transcriptionally, and genetically distinct molecular variants.<sup>3-5</sup> These include the WNT and SHH groups of tumors, which show overexpression of regulators and target genes in the WNT and SHH signaling pathways, respectively,<sup>4</sup>

Yong-Xiao Li, Zhen-Wei Yu and Tao Jiang contributed equally to this work.

This is an open access article under the terms of the Creative Commons Attribution-NonCommercial-NoDerivs License, which permits use and distribution in any medium, provided the original work is properly cited, the use is non-commercial and no modifications or adaptations are made.

© 2018 The Authors. *Cancer Science* published by John Wiley & Sons Australia, Ltd on behalf of Japanese Cancer Association.

Group 3 tumors, in which most tumors show *MYC* amplification and the worst prognosis, and Group 4 tumors, which is the largest subgroup of MB.<sup>4</sup> Subgroup-specific markers to facilitate diagnosis together with precision gene therapy have thus become a critical area in next-generation clinical trials for MB.

Although Group 4 is the largest subtype of MB (up to 30% of tumors),<sup>6</sup> its molecular pathogenesis is the least well understood. The genetic and epigenetic foundations of this group and their clinical significance is incompletely understood.<sup>7-9</sup> Our previous studies showed that MB is an epigenetic disease.<sup>5,10,11</sup> MicroRNA (miR)-449a was identified as a potential epigenetic marker of the Wnt subgroup.<sup>5</sup> However, so far, there are few adequately characterized group-specific epigenetic markers for Group 4.

Our aim was to integrate more potential subtype-specific biomarkers for each subgroup of MBs, especially for Group 4, into the NanoString platform to improve diagnosis efficiency and to find novel therapeutic targets for this tumor. Based on our preliminary result and the criteria in the new WHO classification on MB,<sup>3,5</sup> the custom-designed CodeSet with 11 cancer-related genes and 22 well-characterized group-specific genes were included for the present study.

## 2 | MATERIALS AND METHODS

### 2.1 | Clinicopathologic information

Formalin-fixed, paraffin-embedded samples were obtained from 106 MB in patients from the Third Hospital of Peking University, the Beijing Tiantan Hospital, the Beijing Sanbo Brain Hospital (all Beijing, China), and the Anhui Provincial Hospital (Hefei, China). Tumor samples were collected between September 2009 and December 2011. Each tumor was reviewed by two pathologists (QC and XLQ) for histologic subtyping. Medulloblastomas were histologically classified as classic, desmoplastic nodular, extensive nodular, or large cell/anaplastic variants according to the 2016 WHO classification.<sup>3</sup> The MBs used in this study ( $n = 106$ ) included 56 classic MBs (52.83%), 30 desmoplastic nodular MBs (28.30%), 10 extensive nodular MBs (9.43%), and 10 large cell/anaplastic (9.43%) variants. The mean age of these patients was 8.0 years in 90 children, and 33.4 years in 16 adults. Clinicopathologic information is summarized in Table 1. This study was approved by the Institutional Review Board of Peking University (review reference no. IRB00001052-14003).

### 2.2 | Candidate gene selection

Gene expression analysis was carried out using the classic MB subtyping gene CodeSet, which included 22 well known signature genes for different subgroups,<sup>5,12</sup> as well as 11 additional tumor-related genes. Six of the tumor-related genes (*ALK*, *MYCN*, *TP53*, *GLI1*, *MYC*, and *SNCAIP*) have been reported to be related with different subtypes of this malignant brain tumor, based on various technical assays, and were integrated into the CodeSet here to improve the efficiency of clinical molecular testing as well as strengthen the subtyping fidelity of the NanoString platform.<sup>7,13-18</sup> In addition, some candidates for

therapeutic targets of this tumor, which were screened by our previous study (data not shown), were recruited in the current panel of genes, such as *FGFR1*, *PDGFRA*, and *CCND1*.<sup>19-24</sup> The relationship between these genes and tumor subtyping need to be further elucidated. *HNF4A*, which was recently found to be a specific protein marker in exosomes from supernatant of an MB cell line,<sup>25</sup> as well as *SNCA*, which encodes  $\alpha$ -synuclein, an interactive protein of synphilin-1, which is encoded by *SNCAIP*,<sup>13</sup> were also included in this study.

### 2.3 | RNA isolation and NanoString analysis

Total RNA from formalin-fixed, paraffin-embedded sections extracted from 75 MB samples were analyzed based on the NanoString nCounter Analysis System (NanoString Technologies, Seattle, WA, USA) in the Department of Pathology, Peking University Health Science Center (Beijing, China). All procedures related to mRNA quantification, including sample preparation, hybridization, detection, and scanning, were carried out as previously described.<sup>5</sup> RNA concentration was measured by Qubit (Thermo Fisher). All samples consisted of at least 80% of tumor cells. Normalization of the raw NanoString data was undertaken using nSolver Analysis Software version 2.5 (NanoString Technologies).<sup>12</sup> All statistical analyses were carried out with the R statistical programming environment (version 3.1.1). The Kruskal–Wallis test was used to correlate tumor type and gene expression. The experiment was repeated twice.

### 2.4 | Immunohistochemistry

Formalin-fixed, paraffin-embedded sections from 93 MB were reviewed. Immunohistochemistry (IHC) staining was carried out using  $\alpha$ -synuclein primary mAb (1:1500; 610787; BD Biosciences, San Jose, CA, USA). Staining patterns of  $\alpha$ -synuclein were assessed by two neuropathologists (QC and YFZ) independently, and results were merged to a consensus score. Briefly, the proportion of cells with strong  $\alpha$ -synuclein immunoreactive staining in the cell cytoplasm and/or nucleus in the total tumor area was estimated for each patient.<sup>26</sup> Absence of staining or weak staining was scored as zero. Red blood cells in tumor vessels served as the positive internal control.

### 2.5 | Demethylation treatment of MB cell lines

Three MB cell lines (Daoy, D283, and D341) obtained from the ATCC (Manassas, VA, USA) were treated with 5-aza-2'-deoxycytidine as previously reported,<sup>27</sup> and tested for restoration of *SNCA* gene expression with real-time PCR.

### 2.6 | Sodium bisulfite treatment of DNA followed by methylation-specific PCR and pyrosequencing for detection of *SNCA* promoter methylation in primary MB

Genomic DNA from MB cell lines were treated with sodium bisulfite using the Bisulfite Flash DNA Modification Kit (EpiGentek, Farmingdale,

**TABLE 1** Clinicopathologic information of 106 medulloblastomas (MB)

Case no.	G	A	His	Mol	IHC (%)	MSP	Case no.	G	A	His	Mol	IHC (%)	MSP
MB11	F	5	C	WNT	0	U	MB39	M	5	N/D	Group 4	10	NA
MB20	F	18	C	WNT	0	Me	MB71	M	7	C	Group 4	10	NA
MB58	F	13	C	WNT	0	NA	MB1	M	4	N/D	Group 4	20	U
MB3	F	52	N/D	WNT	5	M	MB42	M	7	N/D	Group 4	30	NA
MB18	F	14	N/D	WNT	5	NA	MB52	M	11	EN	Group 4	30	NA
MB75	F	13	C	WNT	10	NA	MB74	M	4	C	Group 4	35	NA
MB66	F	26	L/A	WNT	NA	NA	MB15	F	9	C	Group 4	40	U
MB68	F	13	C	WNT	NA	NA	MB13	M	22	C	Group 4	60	U
MB2	F	33	C	SHH	0	U	MB36	M	7	N/D	Group 4	60	NA
MB30	M	59	C	SHH	0	U	MB57	F	5	C	Group 4	60	NA
MB38	M	2	L/A	SHH	0	NA	MB9	M	14	C	Group 4	70	NA
MB40	F	1	N/D	SHH	0	NA	MB23	M	6	L/A	Group 4	70	U
MB48	M	7	C	SHH	0	NA	MB34	M	4	EN	Group 4	70	NA
MB51	M	35	N/D	SHH	0	NA	MB24	M	7	C	Group 4	NA	NA
MB64	F	2	C	SHH	0	NA	MB29	M	12	C	Group 4	NA	NA
MB73	M	15	C	SHH	0	NA	MB44	M	14	C	Group 4	NA	NA
MB6	M	4	EN	SHH	5	NA	MB63	M	6	C	Group 4	NA	NA
MB72	F	10	N/D	SHH	15	NA	MB69	M	5	C	Group 4	NA	NA
MB5	M	6	N/D	SHH	20	U	MB70	F	13	L/A	Group 4	NA	NA
MB16	M	38	N/D	SHH	20	U	MB77	F	16	C	NA	0	U
MB43	F	6	L/A	SHH	20	NA	MB81	M	10	C	NA	0	Me
MB12	F	15	C	SHH	60	U	MB82	F	1.5	C	NA	0	U
MB61	F	30	L/A	SHH	NA	NA	MB86	F	3	C	NA	0	U
MB8	F	12	C	Group 3	0	U	MB87	M	3	N/D	NA	0	U
MB14	F	6	L/A	Group 3	0	U	MB88	M	13	N/D	NA	0	U
MB17	M	24	N/D	Group 3	0	U	MB89	M	9	C	NA	0	U
MB31	M	17	C	Group 3	0	NA	MB90	M	3	C	NA	0	Me
MB35	M	7	C	Group 3	0	NA	MB92	M	35	L/A	NA	0	U
MB37	M	5	C	Group 3	0	NA	MB94	F	12	C	NA	0	U
MB41	F	7	C	Group 3	0	NA	MB95	F	5	EN	NA	0	U
MB50	F	12	N/D	Group 3	0	NA	MB101	F	5	C	NA	0	U
MB54	F	11	C	Group 3	0	NA	MB104	M	3	C	NA	0	Me
MB47	M	27	C	Group 3	20	NA	MB106	F	13	EN	NA	0	U
MB33	F	10	N/D	Group 3	50	NA	MB27	M	7	L/A	NA	5	U
MB10	M	1.6	EN	Group 3	60	U	MB80	F	14	N/D	NA	5	Me
MB56	M	2	N/D	Group 3	60	NA	MB91	M	41	EN	NA	5	Me
MB49	F	6	C	Group 3	70	NA	MB103	F	17	C	NA	5	Me
MB7	M	21	C	Group 3	NA	NA	MB84	M	7	C	NA	10	U
MB28	M	7	C	Group 3	NA	NA	MB93	M	8	N/D	NA	20	U
MB62	M	4	C	Group 3	NA	NA	MB98	F	10	EN	NA	20	Me
MB67	M	13	C	Group 3	NA	NA	MB102	F	9	N/D	NA	20	U
MB59	F	5	N/D	Group 4	0	NA	MB96	F	8	N/D	NA	25	U
MB65	F	6	L/A	Group 4	0	NA	MB25	M	5	C	NA	30	NA
MB46	M	6	EN	Group 4	20	NA	MB83	M	2	C	NA	30	U
MB55	F	40	N/D	Group 4	70	NA	MB85	M	16	N/D	NA	30	U
MB4	F	16	C	Group 4	0	NA	MB97	F	6	N/D	NA	30	U

(Continues)

**TABLE 1** (Continued)

Case no.	G	A	His	Mol	IHC (%)	MSP	Case no.	G	A	His	Mol	IHC (%)	MSP
MB19	M	11	C	Group 4	0	U	MB100	F	6	N/D	NA	30	U
MB45	F	10	C	Group 4	0	NA	MB76	M	19	N/D	NA	50	U
MB53	M	7	C	Group 4	0	NA	MB79	F	13	C	NA	50	Me
MB60	F	10	N/D	Group 4	0	NA	MB26	M	4	N/D	NA	70	NA
MB21	M	10	C	Group 4	5	Me	MB99	F	32	C	NA	70	U
MB22	M	10	N/D	Group 4	5	U	MB105	M	8	C	NA	70	U
MB32	M	8	C	Group 4	5	NA	MB78	F	6	EN	NA	80	U

A, age (years); C, classic; EN, extensive nodular; F, female; G, gender; His, Histologic subtype; IHC, positive immunohistochemical staining of  $\alpha$ -synuclein; L/A, large cell/anaplastic; M, male; Me, methylation; Mol, molecular subgroup; MSP, methylation-specific PCR detection of *SNCA* promoter; NA, not available; N/D, nodular/desmoplastic; U, unmethylation.

NY, USA) according to the manufacturer's recommendations.<sup>27</sup> The methylation status of *SNCA* promoter in MB cell lines and 51 primary MBs was evaluated with methylation-specific PCR (MSP) and pyrosequencing (PyroMark Q96; Qiagen, Hilden, Germany) analyses (Table S1). CpGenome universal methylated DNA and universal unmethylated DNA (Millipore, Billerica, MA, USA) were used as methylation and unmethylation controls, respectively. Normal cerebellar tissues were obtained from postmortem brain tissue of four children. All experiments were repeated at least twice.

## 2.7 | Knockdown and overexpression of *SNCA* in MB cells

Daoy, D283, and D341 cells were seeded in 6-well plates at a cell density of  $4 \times 10^4$ . Transfection of three *SNCA* siRNAs (siRNA1, siRNA2, or siRNA3) or siRNA negative control at a final concentration

of 20  $\mu$ mol/L was carried out with Chemifect transfection reagent (Feng Rui, China) according to the manufacturer's recommendations. Transfection of *SNCA* wild-type plasmid (GV219-*SNCA*-wt) and negative control plasmid (GV219) were carried out using Neofect reagent (Lingke Chuangzhi, China) according to the manufacturer's recommendation. Both of the plasmids were given as gifts from Professor Jing Zhang's Parkinson's Disease Laboratory (University of Washington, Seattle, WA, USA). Cells were harvested 24 h after knockdown and overexpression of *SNCA*, followed by quantitative RT-PCR and Western blot analyses for three times, respectively.

## 2.8 | Western blot assay to detect $\alpha$ -synuclein expression in MB cells

Western blot assay was carried out using  $\alpha$ -synuclein primary mAb (1:1000, 610787; BD Biosciences) to detect the  $\alpha$ -synuclein

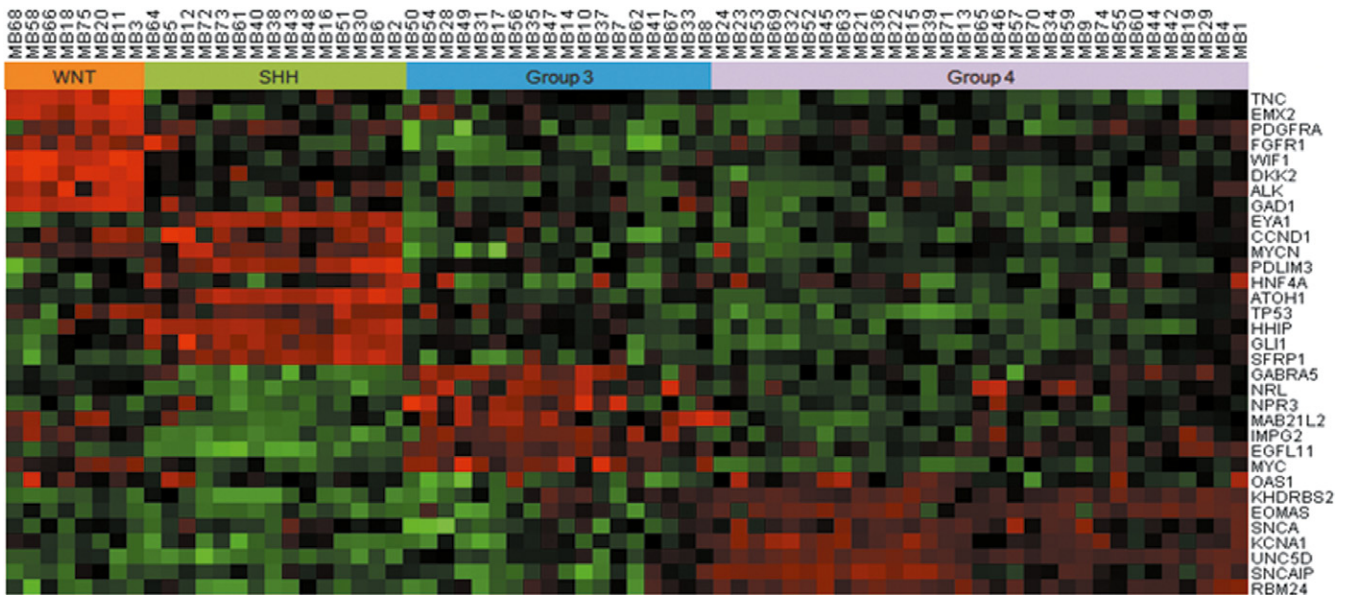


**FIGURE 1** NanoString assay for medulloblastoma subgrouping using the 33 gene CodeSet with the NanoString nCounter Analysis System (NanoString Technologies). Subgroups could be predicted in 96% (72/75) of tumors by non-hierarchical clustering analysis, with 11.11% (8/72) of tumors subgrouped as WNT, 20.83% (15/72) as SHH, 25% (18/72) as Group 3, and 43.06% (31/72) as Group 4. Ten candidate subgroup signature genes were shown to have high subgroup specificity based on the classic gene panel assignment: *PDGFRA*, *FGFR1*, and *ALK* to the WNT group; *CCND1*, *MYCN*, *TP53*, and *GLI1* to the SHH group; *MYC* to Group 3; and *SNCAIP* and *SNCA* to Group 4. Red indicates a high expression level of genes; green indicates low expression level

(A)

Gene	Molecular subtype	AUC	SE	Sensitivity (%)	Specificity (%)	P-value
<i>PDGFR<math>\alpha</math></i>	WNT	0.8594	0.0994	87.50	82.81	$P = 0.0010$
<i>FGFR1</i>	WNT	0.9692	0.0199	100.00	93.85	$P < 0.0001$
<i>ALK</i>	WNT	0.9626	0.0323	85.71	96.92	$P < 0.0001$
<i>CCND1</i>	SHH	0.8259	0.0578	81.25	73.21	$P < 0.0001$
<i>MYCN</i>	SHH	0.9386	0.0273	100.00	76.79	$P < 0.0001$
<i>TP53</i>	SHH	0.8371	0.0533	81.25	82.14	$P < 0.0001$
<i>GLI1</i>	SHH	0.9900	0.0082	100.00	91.07	$P < 0.0001$
<i>MYC</i>	Group 3	0.9033	0.0373	83.33	87.04	$P < 0.0001$
<i>SNCAIP</i>	Group 4	0.9103	0.0325	83.87	82.93	$P < 0.0001$
<i>SNCA</i>	Group 4	0.8875	0.0385	87.10	80.49	$P < 0.0001$

(B)

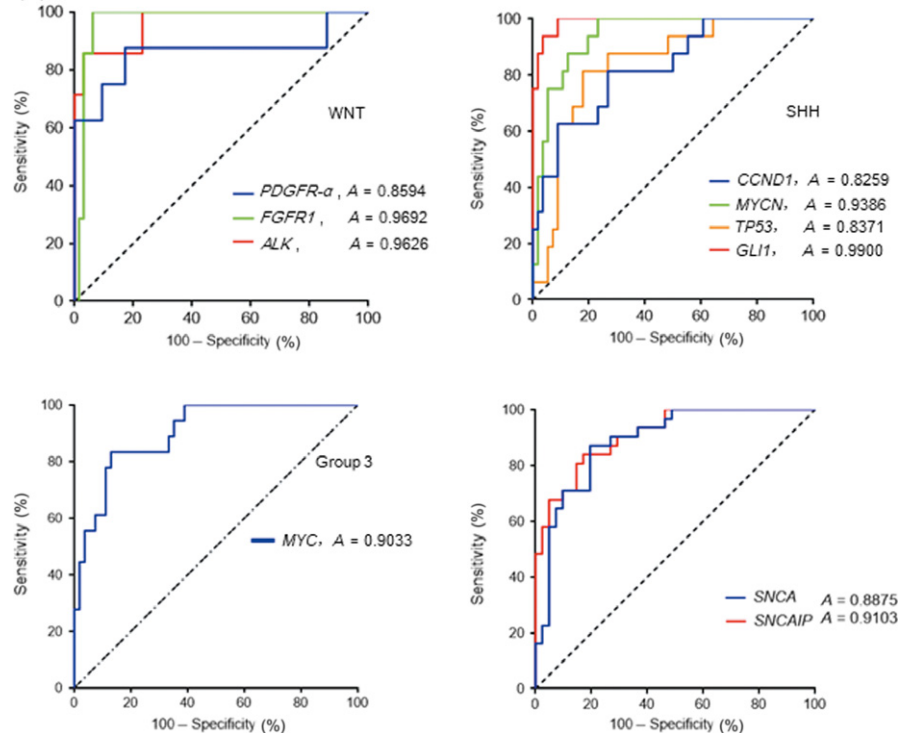


**FIGURE 2** (A) Receiver operating characteristic (ROC) analysis of 10 signature genes assigned to subgroups of medulloblastoma. AUC, area under the ROC curve. (B) ROC curves were generated to evaluate the accuracy of 10 signature genes as diagnostic markers to discriminate different subgroups of tumors. Based on the RNA expression values from the NanoString analysis, each gene in the corresponding subgroup had a higher expression level compared with the other three groups

expression in MB cells (Daoy, D283, and D341) before and after transfection of three *SNCA* siRNAs and GV219-*SNCA* plasmid.  $\beta$ -Actin primary mAb (1:1000, mAbcam 8226; Abcam, Cambridge, MA, USA) was used as the internal control.

## 2.9 | Real-time PCR analysis of *SNCA* mRNA expression after treatment in MB cell lines

First-strand synthesis of cDNA used 5 $\times$  all-in-one RT-mastermix (G486; Applied Biological Materials, Canada) following the manufacturer's instructions. For the qRT-PCR reaction, EvaGreen 2 $\times$  qPCR mastermix-LR (G486; Applied Biological Materials, Richmond, Canada) was used. The protocol was optimized for the 3000p reader (Applied Biosystems, Life Technology). The relative gene expression was calculated for the gene of interest by using the  $\Delta\Delta$ CT method, where cycle threshold values were normalized to  $\beta$ -catenin (Table S1).

## 2.10 | Wound healing and invasion assay of MB cells

Daoy cells were grown to 70–80% confluence. A linear wound was made by scraping a non-opening Pasteur pipette across the confluent cell layer 24 h after transfection of siRNA1, siRNA2, and siRNA3. Cells were washed twice to remove detached cells and debris. The size of these wounds was observed and measured 24 h after scraping. Cell invasion assays was monitored using the Transwell chamber assay. The *SNCA* siRNAs and GV219-*SNCA*-wt plasmid-transfected Daoy cells ( $1 \times 10^5$  cells) were plated on upper chambers with 8- $\mu$ m Transwell filters coated with 25  $\mu$ L Matrigel (1:3; Corning, Corning, NY, USA). The cells were induced to invade towards medium containing 10% FBS in the lower chambers for 24 h. The invaded cells were fixed, stained with 0.1% crystal violet, and analyzed using a bright field microscope. All functional experiments were repeated three times.

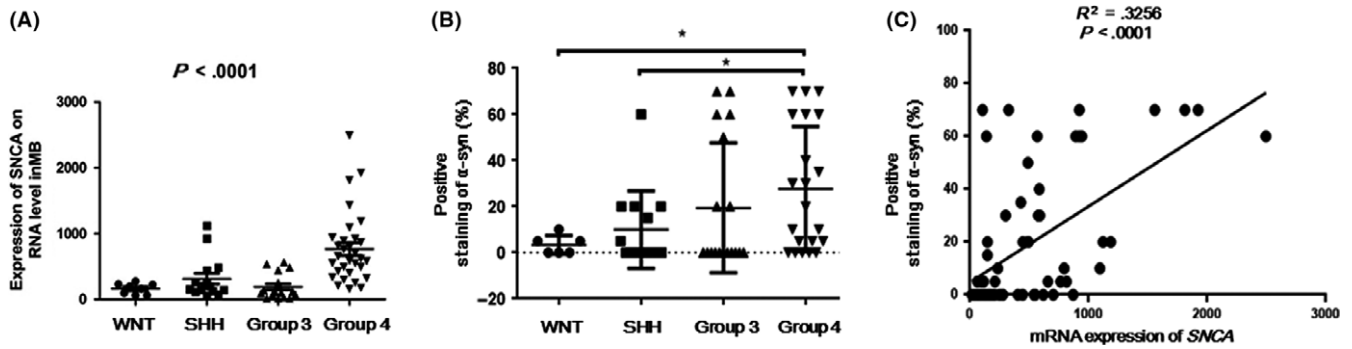


**FIGURE 3** (A) Expression of SNCA in Group 4 medulloblastomas on the RNA level was significantly higher than each of the other three subgroups ( $P < .0001$ ). (B) Significant difference was found in the proportions of  $\alpha$ -synuclein ( $\alpha$ -syn) immunoreactivity in Group 4 compared with WNT and SHH groups.  $*P < .05$ . Protein expression level in Group 4 (means,  $27.62\% \pm 5.932\%$ ;  $n = 21$ ) was higher than that of Group 3 (means,  $19.44\% \pm 6.641\%$ ;  $n = 18$ ), although no statistical significance was identified ( $P = .3632$ ). (C) Expression of SNCA on RNA from NanoString assay and protein levels from immunohistochemistry staining showed significant correlation ( $P < .0001$ ,  $R^2 = .3256$ )

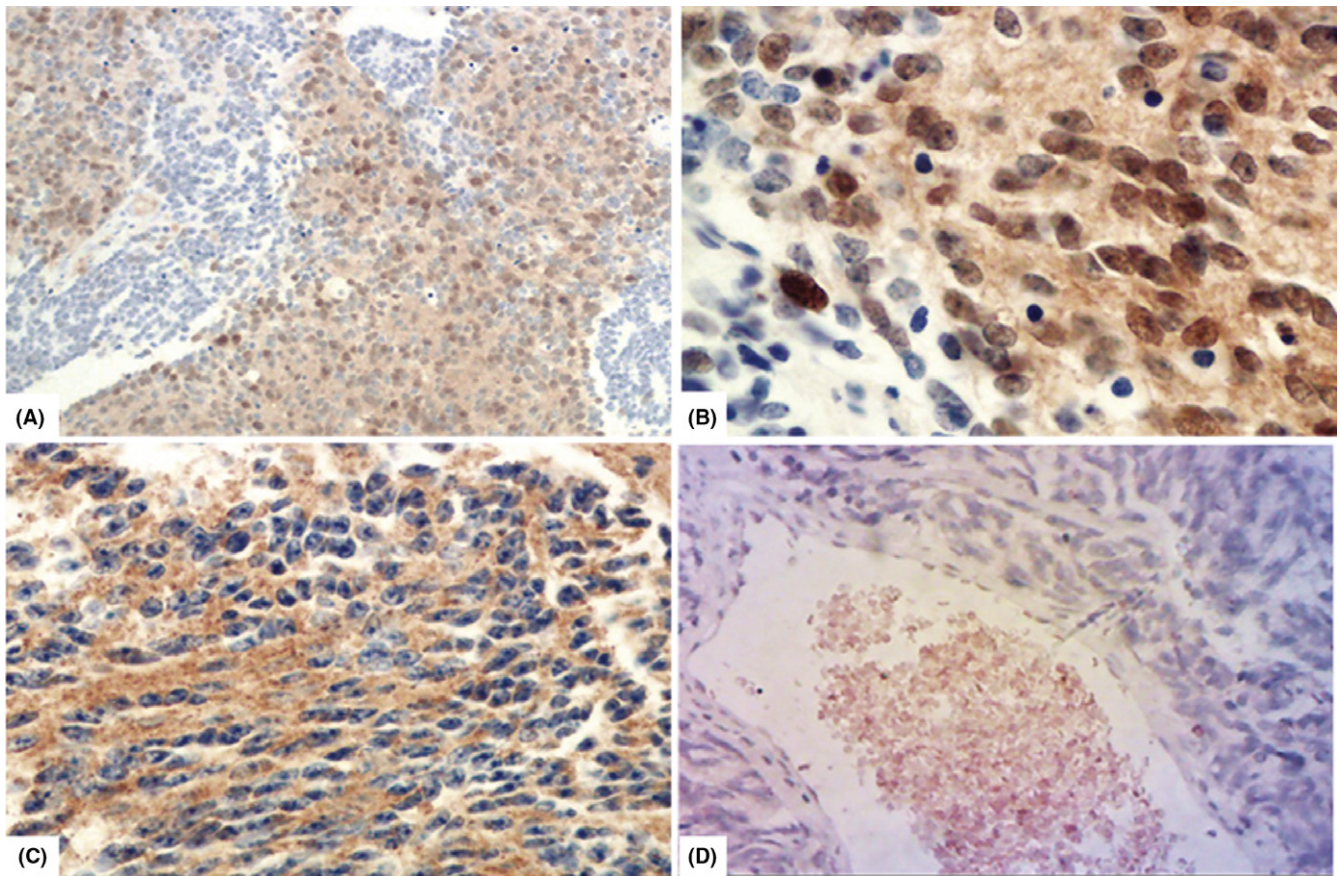


**FIGURE 4** Immunohistochemistry (IHC) staining was carried out in tumor tissues to illustrate protein expression pattern of  $\alpha$ -synuclein in medulloblastomas (MB). (A) Nearly 60% of cells with strong immunoreactivity in the total tumor area was estimated in case number 36 (MB36;  $\times 10$ ,  $\alpha$ -synuclein IHC). (B) Positive staining of  $\alpha$ -synuclein could be identified in the nucleus/cytoplasm of tumor cells under high power view ( $\times 40$ ,  $\alpha$ -synuclein IHC). (C) Positive staining of  $\alpha$ -synuclein could be observed in the cytoplasm of tumor cells in MB15 ( $\times 40$ ,  $\alpha$ -synuclein IHC). (D) Absence of staining, which was scored as zero, was observed in MB19. Red blood cells in tumor vessels served as positive internal control ( $\times 40$ ,  $\alpha$ -synuclein IHC)

## 2.11 | Apoptosis and cell proliferation assay

Apoptosis induction was confirmed by Annexin V-FITC and propidium iodide (PI) detection kit (Jia Mei, China) measured by flow cytometry following the manufacturer's recommended protocol. Flow

cytometry analysis was carried out on a BD FACS Canto II instrument (BD Biosciences, Franklin Lakes, NJ, USA). Data were collected with DIVA software (BD Biosciences, Franklin Lakes) and analyzed with FlowJo software (Tree Star, Ashland, OR, USA) using appropriate controls and gates. Annexin V-positive and PI-negative cells were

**TABLE 2** Significance of molecular changes in medulloblastomas

	Case no.	Percentage	SNCA mRNA by NanoString	$\alpha$ -Syn protein by IHC
Gender	106			
Male	58	58.67	$P = .4749$	$P = .2207$
Female	48	41.33		
Age				
Child	90	84	$P = .5004$	$P = .1987$
Adult	16	16		
Histologic subtype				
Classic	56	52.83	$P = .7065$	$P = .7510$
Nodular/desmoplastic	30	28.3		
Extensive nodular	10	9.43		
Large/anaplastic	10	9.43		
Molecular subgroup by NanoString	72			
WNT	8	11.11	$P < .0001^a$	$P = .0820$
SHH	15	20.83		
Group 3	18	30.56	$P < .0001^b$	$P = .0268^c$
Group 4	31	37.5		
Methylation status of SNCA by MSP	51			
Methylated	11	21.57	$P = .4092$	$P = .1144$
Unmethylated	40	78.43		
Immunostaining of $\alpha$ -syn	93			
>50% +	15	16.13	$P < .0001^d$	
>20% and $\geq$ 50% +	13	13.98		
>5% and $\leq$ 20% +	14	15.05		
$\leq$ 5% +	10	10.75		
–	41	44.09		

+, Positive staining; –, negative staining; IHC, immunohistochemistry staining of  $\alpha$ -synuclein ( $\alpha$ -syn); MSP, methylation-specific PCR detection of SNCA promoter.

<sup>a</sup>mRNA expression levels compared: Group 4 vs Wnt, SHH, and Group 3.

<sup>b</sup>mRNA expression level compared: Group 4 vs three other subgroups of MB.

<sup>c</sup>Protein expression level compared: Group 4 vs WNT and SHH group.

<sup>d</sup>Expression of SNCA on RNA and protein levels showed significant correlation.

in early apoptosis, and cells positive for both Annexin V and PI were either in the late stages of apoptosis or were already dead. Cells transfected by empty vector and normal cells were used as controls. Cell proliferation was detected by CCK-8 (Life Science, USA) according to the manufacturer's instructions.

## 2.12 | Statistical analysis

All statistical analyses was undertaken using the spss 20.0 statistical software package. Results are presented as mean  $\pm$  SEM. Student's *t*-test was used to determine statistical differences between subgroups. Analysis of variance was used to evaluate the relationship between SNCA expression and clinicopathologic characteristics. Spearman's analysis was used to evaluate the correlation between RNA and protein levels of SNCA expression in MB tumors, as well as the consistency of SNCA and SNCAIP expression in these primary

tumors. Other results were evaluated with the independent samples *t*-test. *P*-values  $<.05$  were considered to be statistically significant.

## 3 | RESULTS

### 3.1 | Subgroup assignment of MB and novel signature genes specific to each group identified by NanoString assay

Our previous study validated the reliability of the NanoString assay for MB subgrouping in 45 Chinese patients using the 22 classic gene CodeSet with the NanoString nCounter Analysis System (NanoString Technologies).<sup>5</sup> To further integrate more subgroup-specific genes recruited by the 2016 WHO classification and other studies using various techniques into one platform, and to find therapeutic targets in the current study, we assigned molecular subgroups in 72 primary

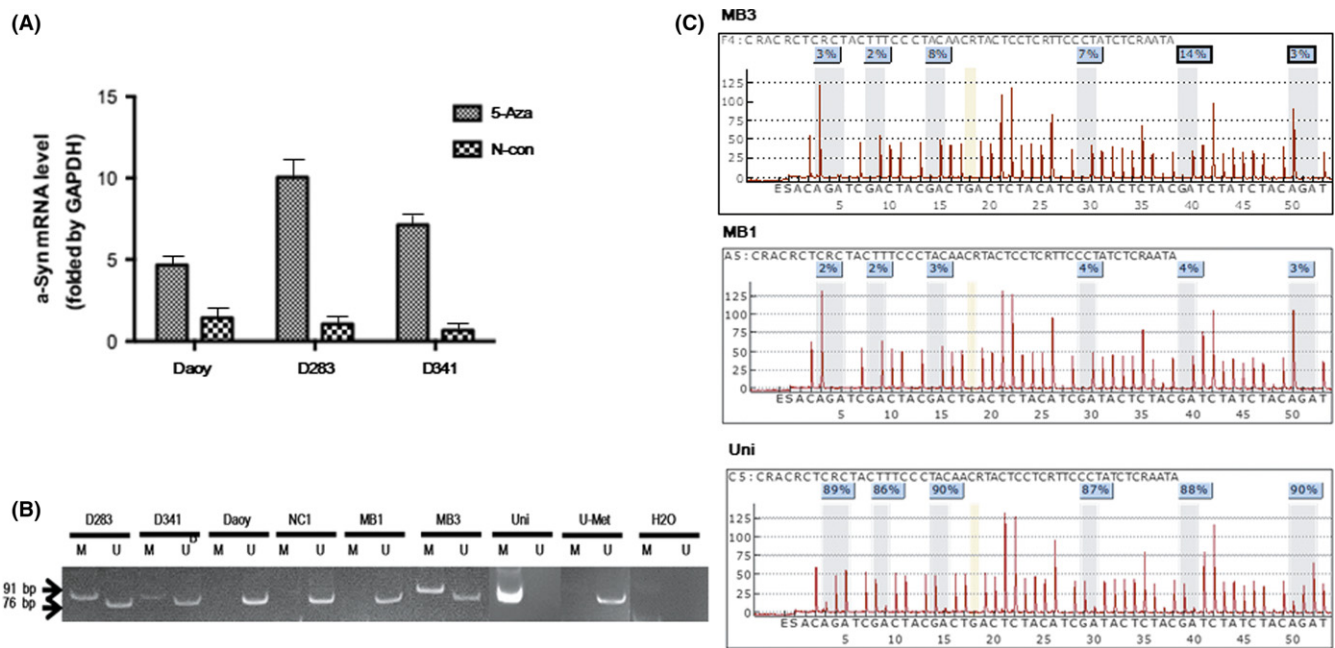


**FIGURE 5** (A) Demethylation reagent (5-aza-2'-deoxycytidine [5-Aza]) treatment reversed the expression levels of the *SNCA* gene in medulloblastoma (MB) cell lines (Daoy, D283, and D341) detected by real-time PCR.  $\alpha$ -Syn,  $\alpha$ -synuclein; N-con, negative control. (B) *SNCA* promoter CpG islands were evaluated with methylation-specific PCR. Hypermethylation was observed in D283 and D341 cells as well as primary MB (MB3). No methylation was detected in Daoy cells or primary tumor (MB1). An unmethylated band was detected in all cell lines and primary tumors, including D283 and D341 cells, and in the hypermethylated tumor (MB3). No methylation was detected in normal cerebellar tissue (NC1). (C) *SNCA* promoter CpG islands were analyzed by pyrosequencing. Higher frequency of methylation ( $\geq 5\%$ ) can be identified in three of six CpG sites in the promoter region of *SNCA* in MB3. However, the frequency of methylation of the other three CpG sites is low ( $< 5\%$ ). No hypermethylation was detected in MB1. H<sub>2</sub>O, negative control; Uni, universal methylated DNA was used as positive control

MB with a larger custom-designed CodeSet, which contained 33 genes including 11 additional candidate subgroup signature genes. Current results showed that the MB subgroup could be predicted in a larger cohort of tumors (96%, 72/75) by non-hierarchical clustering analysis, with 11.11% (8/72) of tumors subgrouped as WNT, 20.83% (15/72) as SHH, 25% (18/72) as Group 3, and 43.06% (31/72) as Group 4 (Table 1, Figure 1). Analysis and normalization of raw NanoString data using nSolver Analysis Software version 2.5 (NanoString Technologies) showed a “quantification control (QC) flag” in 3/75 (4%) of cases (MB25, MB26, and MB27), which means our current NanoString assay was unable to provide a high confidence for subgroup assignment in these three cases (Table S2).

Among the 11 candidate signature genes, 10 were shown to have higher expression and a close relationship with different subgroups based on the classic panel gene assignment: *PDGFRA*, *FGFR1*, and *ALK* are associated with the WNT group; *CCND1*, *MYCN*, *TP53*, and *GLI1* are associated with the SHH group; *MYC* is associated with Group 3; and *SNCAIP* and *SNCA* are associated with Group 4 (Figure 1).

### 3.2 | Receiver operating characteristic curves of 10 newly identified subtyping genes

To evaluate the accuracy of these 10 genes as diagnostic markers to discriminate different subgroup tumors, receiver operating characteristic (ROC) curves were generated based on the higher RNA expression values from the NanoString analysis for each gene in the

corresponding subgroup compared with the other three groups. The area under the ROC curves were: 0.8594, 0.9692, and 0.9626 for *PDGFRA*, *FGFR1*, and *ALK* in the WNT group, respectively; 0.8259, 0.9386, 0.8371, and 0.9900 for *CCND1*, *MYCN*, *TP53*, and *GLI1* in the SHH group, respectively; 0.9033 for *MYC* in Group 3; and 0.9103 and 0.8875 for *SNCAIP* and *SNCA* in Group 4, respectively (Figure 2). Among these genes, *SNCA* is reported for the first time to be related to Group 4 MB, with high sensitivity (87.1%) and high specificity (80.49%; Figure 2A). The expression of *SNCA* in Group 4 on the RNA level was significantly higher than in WNT, SHH, and Group 3 ( $P < .0001$ ; Figure 3), indicating that *SNCA* is a diagnostic marker with high sensitivity and specificity for subtyping MB on the RNA level.

### 3.3 | Alpha-synuclein expression and its association with MB subgroups

To illustrate protein expression of  $\alpha$ -synuclein encoded by *SNCA* in MB, IHC staining was undertaken in 93 MBs, and showed cytoplasmic and/or nuclear staining in differing proportions of the tumor area (Table 1; Figure 4). Among these MBs, 59 cases have been detected by the NanoString platform and were assigned with molecular subgroups (Table 1). The proportions of  $\alpha$ -synuclein immunoreactivity in Group 4 was significantly higher compared with WNT and SHH groups ( $P = .0413$  and  $.0381$ , respectively, *t*-test; Table 2, Figure 3B). It was also higher in Group 4 (with means of



27.62%  $\pm$  5.932%,  $n = 21$ ) than that of Group 3 (with means of 19.44%  $\pm$  6.641%,  $n = 18$ ), although the difference was not statistically significant in our cohort ( $P = .3632$ ,  $t$ -test; Figure 3B). The *SNCA* gene expression on RNA and protein levels showed significant correlation ( $P < .0001$ ,  $R^2 = 0.3256$ ; Table 2, Figure 3C). RNA expression of *SNCA* was also closely related with that of *SNCAIP*, based on our NanoString data ( $P < .0001$ ; Figure S1). Both of these molecules are specific markers with relatively high expression level in Group 4 MBs (Figure 2).

### 3.4 | *SNCA* promoter methylation status in MB

Previous studies have shown that expression of *SNCA* is regulated by hypermethylation of the CpG island in its promoter region in various human cancers.<sup>28-31</sup> Demethylation drug treatment in MB cells showed reversed expression of this gene, suggesting that the silenced expression of *SNCA* might be due to epigenetic regulation, including DNA hypermethylation (Figure 5A). To analyze the methylation status of the *SNCA* promoter CpG island in MB, three MB cell lines (Daoy, D283, and D341) and 51 primary tumors, for which DNA was available, were evaluated with MSP and pyrosequencing. Hypermethylation was observed in D283 and D341 cells as well as in 21.57% (11/51) of primary MB by MSP (Figure 5B). No methylation was detected in Daoy cells. An unmethylated band was detected in all cell lines and primary tumors, including D283 and

D341 cells and in the hypermethylated primary MBs, indicating that hypermethylation in all of these tumors is incomplete. This result is consistent with our data from pyrosequencing analyses showing the frequency of hypermethylation is rather low in some CpG sites of the promoter region (<5%; Figure 5C), implying that epigenetic mechanisms other than DNA hypermethylation might play the key role in the regulation of *SNCA* expression (e.g. histone modification).

### 3.5 | Capacity for migration and invasion in MB cells after knockdown and overexpression of $\alpha$ -synuclein, respectively

To explore the function of *SNCA* in MB cells, specific knockdown assays by siRNA transfection were carried out. Expression of *SNCA* was inhibited by siRNA (Figure 6). After transfection, the invasion ability of MB was significantly increased compared with the negative control. In contrast, overexpression of *SNCA* can decrease the invasion ability (Figure 7A). Wound healing assays showed that the migration ability was also increased after transfection of *SNCA* siRNA (Figure 7B).

### 3.6 | Cell apoptotic and proliferation ability

To evaluate the effect of *SNCA* on apoptosis in MB cells, the Annexin V/PI detection assay was carried out (Figure 8). The

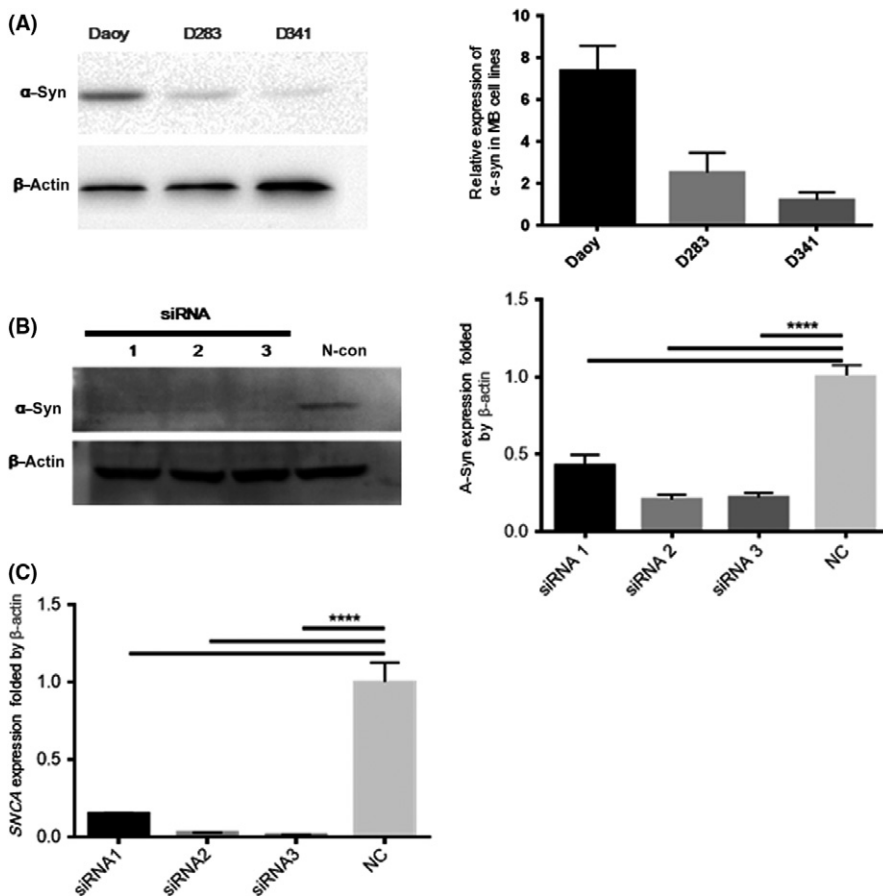


**FIGURE 6** Specific knockdown assays by *SNCA* siRNA transfection were carried out in medulloblastoma cells. (A) Expression of  $\alpha$ -synuclein ( $\alpha$ -Syn) in medulloblastoma cell lines (Daoy, D283, and D341) were detected by Western blot analysis, showing that the expression level of  $\alpha$ -syn in Daoy is higher than D283 and D341. (B) Alpha-synuclein expression in Daoy cells was inhibited by transfection of siRNA for 24 h, analyzed by Western blot. (C) *SNCA* gene expression in Daoy cells was reduced by >50% after the transfection of siRNA1, siRNA2, and siRNA3 for 24 h, identified by real-time PCR. The experiment was repeated at least twice.  $\beta$ -Actin, housekeeping gene; N-con, negative siRNA control

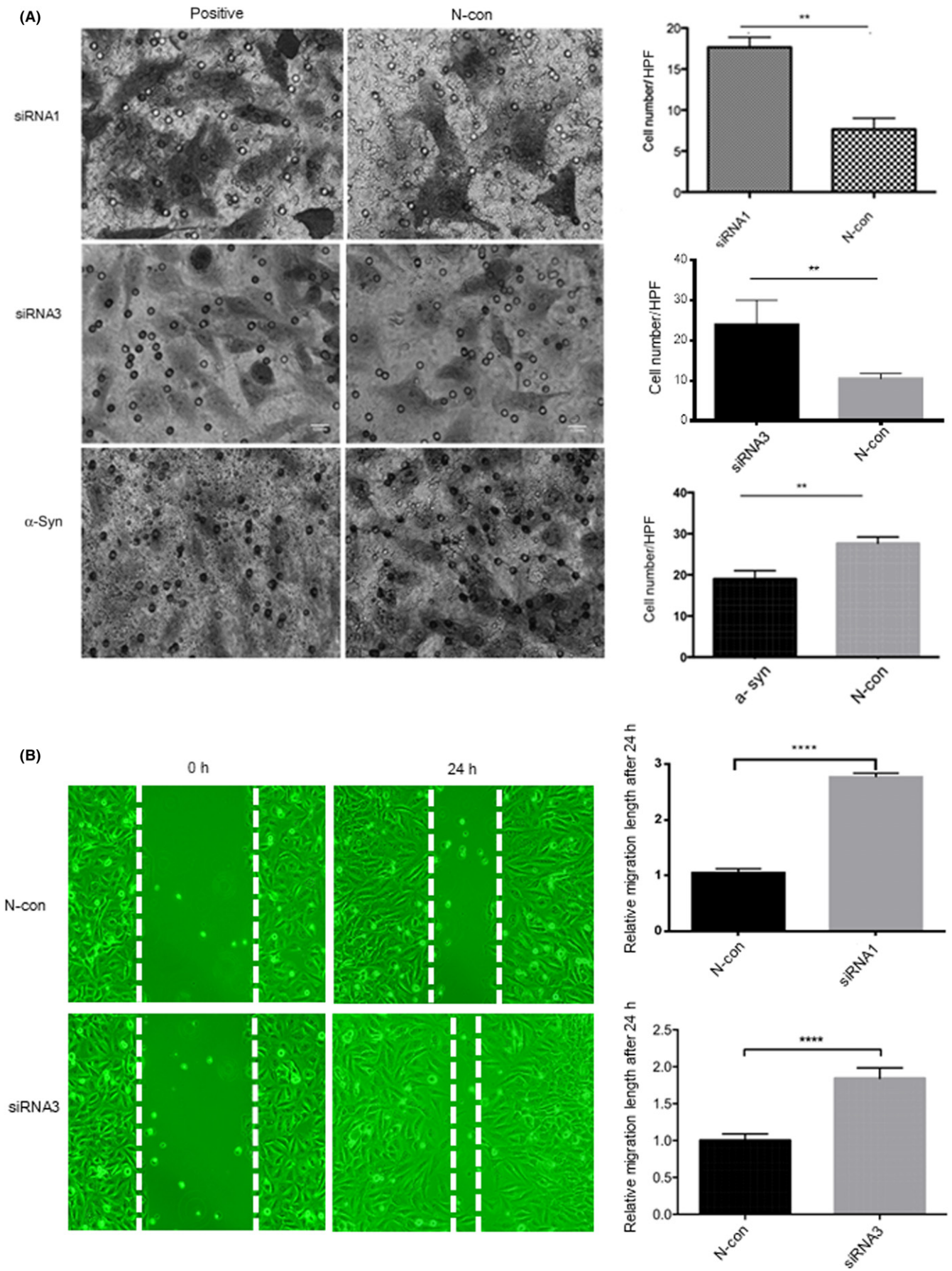


**FIGURE 7** (A) Transwell invasion assay. Daoy cells after transfection of *SNCA* siRNA1, siRNA2, siRNA3, or GV219-*SNCA*-wt for 24 h. After knockdown transfection, the invasion ability of Daoy cells after transfection of *SNCA* siRNA was significantly increased compared with the negative siRNA control (N-con). After overexpression of *SNCA*, the invasion ability decreased significantly. HPF, high power field ( $\times 40$ ). (B) Wound healing assay. Daoy cells showed that the migration ability was significantly increased after transfection of *SNCA* siRNA for 24 h compared with N-con. Low power field ( $\times 4$ ). \*\* $P < .01$ ; \*\*\*\* $P < .0001$ ;  $\alpha$ -Syn, GV219-*SNCA*-wt vector transfection

proportions of MB cells in early apoptosis and late stages of apoptosis, or already dead, were significantly higher than those of the normal cells and negative control ( $P < .0001$ ). There was no significant difference before or after overexpression of *SNCA* in tumor cell proliferation (Figure S2), indicating that *SNCA* can improve the apoptotic activity of MB cells rather than cell proliferation.

#### 4 | DISCUSSION

In the current study, novel subtype-specific diagnostic and/or therapeutic markers for each subgroup of MB, especially for Group 4, the largest group, were explored. *SNCA* was identified for the first time as the signature marker in Group 4 with high specificity and sensitivity. Regulation mechanism and functional studies were undertaken, focused on this gene. Some well-known subgroup-specific biomarkers revealed by various techniques and included in the new WHO classification, such as *P53*, *NMYC*, and *MYC*, were also integrated into our platform to improve clinical testing efficiency.

It is well known that increased expression of *SNCA* is closely correlated with increased risk of developing Parkinson's disease (PD).<sup>32</sup> Recently, it was reported that polymorphism in the *SNCA* gene is associated with PD phenotype.<sup>33</sup> Non-viral vectors that can deliver siRNA against *SNCA* has been developed and can prevent PD-like symptoms both in vitro and in vivo,<sup>34</sup> indicating that *SNCA* can be the potential target of gene therapy. Co-expression of  $\alpha$ -synuclein and synphilin-1, which are encoded by *SNCA* and *SNCAIP*, respectively, favor the formation of Lewy bodies in the brain of patients with PD.<sup>35,36</sup> Interestingly, the expression of  $\alpha$ -synuclein could also be identified diffusely in tumors showing neuronal differentiation, including MB.<sup>26,37</sup> Although the duplication of *SNCAIP* has been reported to be a somatic event highly specific to Group 4 MB,<sup>13</sup> so far the relationship between *SNCA* and MB subtype has not been clarified. Based on the present data from subtyping, our study then focused on the *SNCA* gene in the largest subgroup of MB.

The RNA expression level of *SNCA* in Group 4 detected in the current study was significantly higher than each of the other three subgroups, and the area under the ROC curve was rather high,

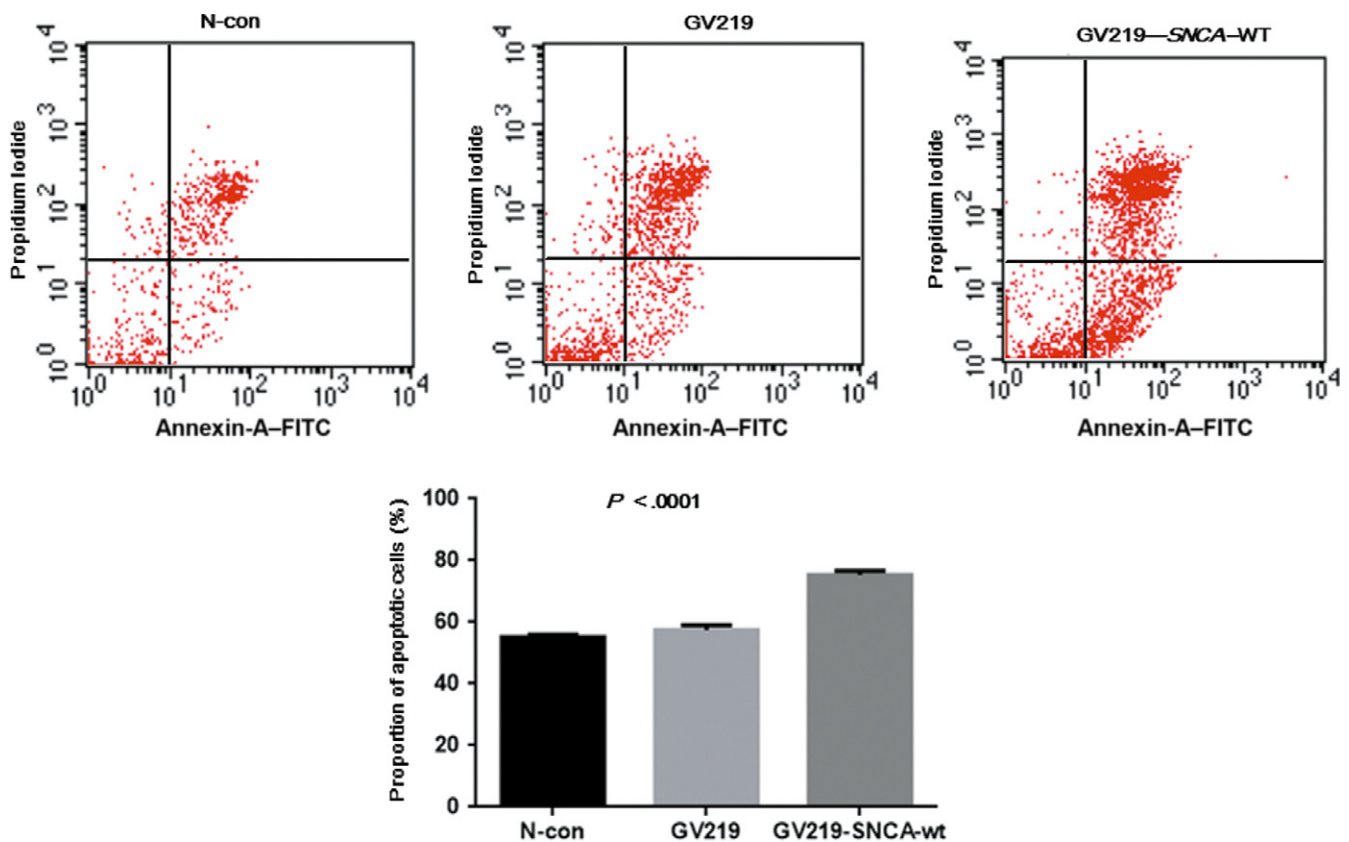


**FIGURE 8** Quantification of apoptotic human medulloblastoma cells with and without *SNCA* overexpression was determined by the Annexin V-propidium iodide method. The percentages of cells that are in early and late stages of apoptosis or already dead are significantly higher in cells with *SNCA* overexpression than in those without gene overexpression.  $P < .0001$ . N-con, negative control

indicating *SNCA* is a diagnostic marker for Group 4 MB with high sensitivity and specificity on the mRNA level. In addition,  $\alpha$ -synuclein protein expression in MB showed significantly higher in the proportions of  $\alpha$ -synuclein immunoreactivity in Group 4 compared with WNT and SHH groups. The protein expression level in Group 4 was also higher than that of Group 3, although the difference was not significant, which might be due to the limited case numbers. *SNCA* mRNA expression level and the proportion of positive staining for  $\alpha$ -synuclein protein showed statistically significant correlation, supporting that *SNCA* could serve as a marker in MB subtyping not only on the RNA level but also on the protein level.

It has been reported that *SNCA* expression is regulated by epigenetic mechanisms in a series of human cancers, including cholangiocarcinoma,<sup>28</sup> colorectal cancer,<sup>29,30</sup> and non-Hodgkin's lymphoma.<sup>31</sup> Bethge et al<sup>31</sup> reported that *SNCA* methylation might be suitable for early detection and monitoring of non-Hodgkin's lymphoma. In our cohort, demethylation treatment could reverse the gene's expression on the mRNA level in all three MB cell lines. Hypermethylation could be detected in some CpG sites of the promoter region, but the frequency of other CpG sites was rather low, shown by pyrosequencing analysis. That may explain the poor correlation between DNA methylation status from MSP and gene expression analyses (Table 2), indicating that *SNCA* expression might be regulated indirectly by epigenetic mechanisms other than DNA methylation, such as histone modification.

Alpha-synuclein aggregation was recently identified as essential to apoptotic neurons in PD.<sup>38</sup> It was also observed to be downregulated by miR-153-3p and miR-205-5p in neuroblastoma cells, suggesting its potential as a tumor suppressor.<sup>39</sup> In the present study, the anti-apoptotic function and invasion ability of MB cells, rather than cell proliferation, were increased after *SNCA* siRNA transfection, but decreased after overexpression of the gene, indicating the potential tumor suppressor function of *SNCA* in MB. Expression of *SNCA* was observed to have a close relationship with *SNCAIP* in MB (Figure S1), which has been reported to be related with various tumors.<sup>40,41</sup> Future study will be required to understand the mechanism of the synergetic effect between *SNCA* and *SNCAIP* on MB tumor invasion as well as apoptosis in vitro and in vivo.

Recently, each subgroup of MB was split further based on comprehensive molecular profiling that can improve disease risk stratification and inform treatment decisions.<sup>42,43</sup> In order to integrate more diagnostic markers and candidates for therapeutic targets of this tumor into one testing platform, we also investigated the correlation of several additional candidate signature genes with subgroups of MB. Some of these markers, such as *ALK* in the WNT group, *TP53*, *NMYC*, and *GLI1* in the SHH group, *MYC* in Group 3, and *SNCAIP* in Group 4, have been identified in various studies using different methods, which strongly supports the results from the NanoString assay in the current study.<sup>7,13-18</sup> Furthermore, we identified several novel MB subgroup markers, including *FGFR1* and *PDGFRA* in the WNT group and *CCND1* in the SHH group. These three genes have all been reported to be potential targets for gene therapy in various tumors.<sup>20-22</sup> It is hoped that further exploration in vitro and

in vivo will reveal their therapeutic value in specific subtypes of MB. *PDGFRA* was assigned to the WNT group in the present cohort, whereas it has been classified to the SHH group in another report.<sup>7</sup> The inconsistency between different studies could be due to variations from different races or technique platforms, which need larger cohorts of samples to clarify.

In summary, we showed for the first time that *SNCA* is a Group 4-related diagnostic marker with both high sensitivity and specificity in MB. *SNCA* expression might be regulated indirectly with epigenetic mechanisms rather than DNA hypermethylation. Further survival analyses will clarify its prognostic value for MB patients. In addition, the NanoString gene expression assay enriched with the 33 custom-designed gene CodeSet showed excellent efficiency for MB subgroup assignment and potential biomarker identification. Our knowledge of MB in this study will shed new light on clinical usage of molecular subtyping of MB and, ultimately, benefit the patients.

## ACKNOWLEDGMENTS

This work was supported by the National Natural Science Foundation of China (Grant Nos. 81101900 and 30540008) and the Clinicopathologic Innovation Fund from Peking University Third Hospital, Peking University Health Science Center (to Qing Chang).

## CONFLICT OF INTEREST

The authors have no conflict of interest.

## ORCID

Qing Chang  <http://orcid.org/0000-0001-5138-8760>

## REFERENCES

- Kim SY, Sung KW, Hah JO, et al. Reduced-dose craniospinal radiotherapy followed by high-dose chemotherapy and autologous stem cell rescue for children with newly diagnosed high-risk medulloblastoma or supratentorial primitive neuroectodermal tumor. *Korean J Hematol*. 2010;45:120-126.
- Packer RJ, Gajjar A, Vezina G, et al. Phase III study of craniospinal radiation therapy followed by adjuvant chemotherapy for newly diagnosed average-risk medulloblastoma. *J Clin Oncol*. 2006;24:4202-4208.
- Louis DN, Perry A, Reifenberger G, et al. The 2016 world health organization classification of tumors of the central nervous system: a summary. *Acta Neuropathol*. 2016;131:803-820.
- Kool M, Korshunov A, Remke M, et al. Molecular subgroups of medulloblastoma: an international meta-analysis of transcriptome, genetic aberrations, and clinical data of WNT, SHH, Group 3, and Group 4 medulloblastomas. *Acta Neuropathol*. 2012;123:473-484.
- Li Y, Jiang T, Shao L, et al. Mir-449a, a potential diagnostic biomarker for WNT group of medulloblastoma. *J Neurooncol*. 2016;129:423-431.
- Taylor MD, Northcott PA, Korshunov A, et al. Molecular subgroups of medulloblastoma: the current consensus. *Acta Neuropathol*. 2012;123:465-472.
- Northcott PA, Korshunov A, Witt H, et al. Medulloblastoma comprises four distinct molecular variants. *J Clin Oncol*. 2011;29:1408-1414.

8. Ellison DW, Dalton J, Kocak M, et al. Medulloblastoma: clinicopathological correlates of SHH, WNT, and non-SHH/WNT molecular subgroups. *Acta Neuropathol.* 2011;121:381-396.
9. Ramaswamy V, Remke M, Bouffet E, et al. Recurrence patterns across medulloblastoma subgroups: an integrated clinical and molecular analysis. *Lancet Oncol.* 2013;14:1200-1207.
10. Pang JC, Chang Q, Chung YF, et al. Epigenetic inactivation of DLC-1 in supratentorial primitive neuroectodermal tumor. *Hum Pathol.* 2005;36:36-43.
11. Chang Q, Pang JC, Li KK, Poon WS, Zhou L, Ng HK. Promoter hypermethylation profile of RASSF1A, FHIT, and sFRP1 in intracranial primitive neuroectodermal tumors. *Hum Pathol.* 2005;36:1265-1272.
12. Northcott PA, Shih DJ, Remke M, et al. Rapid, reliable, and reproducible molecular sub-grouping of clinical medulloblastoma samples. *Acta Neuropathol.* 2012;123:615-626.
13. Northcott PA, Shih DJ, Peacock J, et al. Subgroup-specific structural variation across 1,000 medulloblastoma genomes. *Nature.* 2012;488:49-56.
14. Cho YJ, Tsherniak A, Tamayo P, et al. Integrative genomic analysis of medulloblastoma identifies a molecular subgroup that drives poor clinical outcome. *J Clin Oncol.* 2011;29:1424-1430.
15. Kool M, Koster J, Bunt J, et al. Integrated genomics identifies five medulloblastoma subtypes with distinct genetic profiles, pathway signatures and clinicopathological features. *PLoS One.* 2008;3:e3088.
16. Lastowska M, Trubicka J, Niemira M, et al. ALK expression is a novel marker for the WNT-activated type of pediatric medulloblastoma and an indicator of good prognosis for patients. *Am J Surg Pathol.* 2017;41:781-787.
17. Li KK, Lau KM, Ng HK. Signaling pathway and molecular subgroups of medulloblastoma. *Int J Clin Exp Pathol.* 2013;6:1211-1222.
18. Min HS, Lee JY, Kim SK, Park SH. Genetic grouping of medulloblastomas by representative markers in pathologic diagnosis. *Transl Oncol.* 2013;6:265-272.
19. Emmenegger BA, Hwang EI, Moore C, et al. Distinct roles for fibroblast growth factor signaling in cerebellar development and medulloblastoma. *Oncogene.* 2013;32:4181-4188.
20. Faria CC, Golbourn BJ, Dubuc AM, et al. Foretinib is effective therapy for metastatic sonic hedgehog medulloblastoma. *Cancer Res.* 2015;75:134-146.
21. Gravina GL, Mancini A, Sanita P, et al. Erratum to: KPT-330, a potent and selective exportin-1 (XPO-1) inhibitor, shows antitumor effects modulating the expression of cyclin D1 and survivin in prostate cancer models. *BMC Cancer.* 2016;16:8.
22. Katoh M. FGFR inhibitors: effects on cancer cells, tumor microenvironment and whole-body homeostasis (Review). *Int J Mol Med.* 2016;38:3-15.
23. Li M, Lockwood W, Zielenska M, et al. Multiple CDK/CYCLIND genes are amplified in medulloblastoma and supratentorial primitive neuroectodermal brain tumor. *Cancer Genet.* 2012;205:220-231.
24. MacDonald TJ, Brown KM, LaFleur B, et al. Expression profiling of medulloblastoma: PDGFRA and the RAS/MAPK pathway as therapeutic targets for metastatic disease. *Nat Genet.* 2001;29:143-152.
25. Epple LM, Griffiths SG, Dechkovskaia AM, et al. Medulloblastoma exosome proteomics yield functional roles for extracellular vesicles. *PLoS One.* 2012;7:e42064.
26. Fung KM, Rorke LB, Giasson B, Lee VM, Trojanowski JQ. Expression of alpha-, beta-, and gamma-synuclein in glial tumors and medulloblastomas. *Acta Neuropathol.* 2003;106:167-175.
27. Shao LW, Pan Y, Qi XL, et al. ATRX loss in adult supratentorial diffuse astrocytomas correlates with p53 over expression and IDH1 mutation and predicts better outcome in p53 accumulated patients. *Histol Histopathol.* 2016;31:103-114.
28. Andresen K, Boberg KM, Vedeld HM, et al. Four DNA methylation biomarkers in biliary brush samples accurately identify the presence of cholangiocarcinoma. *Hepatology.* 2015;61:1651-1659.
29. Lind GE, Danielsen SA, Ahlquist T, et al. Identification of an epigenetic biomarker panel with high sensitivity and specificity for colorectal cancer and adenomas. *Mol Cancer.* 2011;10:85.
30. Li WH, Zhang H, Guo Q, et al. Detection of SNCA and FBN1 methylation in the stool as a biomarker for colorectal cancer. *Dis Markers.* 2015;2015:657570.
31. Bethge N, Lothe RA, Honne H, et al. Colorectal cancer DNA methylation marker panel validated with high performance in Non-Hodgkin lymphoma. *Epigenetics.* 2014;9:428-436.
32. Soldner F, Stelzer Y, Shivalila CS, et al. Parkinson-associated risk variant in distal enhancer of alpha-synuclein modulates target gene expression. *Nature.* 2016;533:95-99.
33. Zheng J, Yang X, Zhao Q, et al. Festination correlates with SNCA polymorphism in Chinese patients with Parkinson's disease. *Parkinsons Dis.* 2017;2017:3176805.
34. Javed H, Menon SA, Al-Mansoori KM, et al. Development of nonviral vectors targeting the brain as a therapeutic approach for Parkinson's disease and other brain disorders. *Mol Ther.* 2016;24:746-758.
35. Engelender S, Kaminsky Z, Guo X, et al. Synphilin-1 associates with alpha-synuclein and promotes the formation of cytosolic inclusions. *Nat Genet.* 1999;22:110-114.
36. Chung KK, Zhang Y, Lim KL, et al. Parkin ubiquitinates the alpha-synuclein-interacting protein, synphilin-1: implications for Lewy-body formation in Parkinson disease. *Nat Med.* 2001;7:1144-1150.
37. Kawashima M, Suzuki SO, Doh-ura K, Iwaki T. alpha-Synuclein is expressed in a variety of brain tumors showing neuronal differentiation. *Acta Neuropathol.* 2000;99:154-160.
38. Jiang P, Gan M, Yen SH, McLean PJ, Dickson DW. Histones facilitate alpha-synuclein aggregation during neuronal apoptosis. *Acta Neuropathol.* 2017;133:547-558.
39. Patil KS, Basak I, Pal R, et al. A proteomics approach to investigate miR-153-3p and miR-205-5p targets in neuroblastoma cells. *PLoS One.* 2015;10:e0143969.
40. Liu H, Wang Y, Sharma A, et al. Derivatives containing both coumarin and benzimidazole potently induce caspase-dependent apoptosis of cancer cells through inhibition of PI3K-AKT-mTOR signaling. *Anticancer Drugs.* 2015;26:667-677.
41. Fridley BL, Ghosh TM, Wang A, et al. Genome-wide study of response to platinum, taxane, and combination therapy in ovarian cancer: in vitro phenotypes, inherited variation, and disease recurrence. *Front Genet.* 2016;7:37.
42. Northcott PA, Buchhalter I, Morrissy AS, et al. The whole-genome landscape of medulloblastoma subtypes. *Nature.* 2017;547:311-317.
43. Schwalbe EC, Lindsey JC, Nakjang S, et al. Novel molecular subgroups for clinical classification and outcome prediction in childhood medulloblastoma: a cohort study. *Lancet Oncol.* 2017;18:958-971.

## SUPPORTING INFORMATION

Additional Supporting Information may be found online in the supporting information tab for this article.

**How to cite this article:** Li Y-X, Yu Z-W, Jiang T, et al. SNCA, a novel biomarker for Group 4 medulloblastomas, can inhibit tumor invasion and induce apoptosis. *Cancer Sci.* 2018;109:1263-1275. <https://doi.org/10.1111/cas.13515>